



A Fluorescent Visual Proton Donor and Photoacid Sterilant Based on Sulfonate-conjugated BODIPY

Abbas Mohammed Ali¹ · Jian Shao¹ · Jia-Xin Wang¹ · Qiu-Yun Chen¹ · Yang Li¹ · Ling-Ling Qu¹ 

Received: 18 October 2020 / Accepted: 5 January 2021 / Published online: 15 January 2021
© The Author(s), under exclusive licence to Springer Science+Business Media, LLC part of Springer Nature 2021

Abstract

Increasing acidity is an effective method for bacterial inactivation by inhibiting the synthesis of intracellular proteins at low pH. Photo-driven proton release probe can be used for the measurement of proton in hydrophobic condition. To develop fluorescent proton donor, two boron dipyrromethene derivatives (BDP-S and BDP-S2) were characterized by spectroscopic methods. Irradiation of BDP-S by white LED light resulted in efficient generation of acidic species with changes of fluorescence emission. The linear relationship between the pH value and the fluorescence intensity of BDP-S was obtained, indicating that BDP-S is a fluorescent visual proton donor. Light-induced antibacterial results indicate that BDP-S can significantly inhibit the growth of *E. coli*. The results prove that BDP-S is a very promising photoacid sterilant.

Keywords BODIPY · Antibacterial · Proton donor · Photoacid generator

Introduction

The effectiveness of traditional antibiotics is decreasing due to variations of pathogens and enhancement of drug resistance in recent years. This has given rise to the search for a more effective way of bacterial inactivation. Light-driven bacterial inactivation has become the main treatment method in the fields of biomedicine, environmental science and materials chemistry because of its non-invasiveness, less toxicity and low drug resistance [1–4]. Photo-driven antibacterial by photoacid is a promising approach in photo-driven bacteria killing [5]. Photoacid generators (PAGs) are a class of compounds that undergo dissociation or rearrangement reactions upon illumination, resulting in acidic species eventually [6–10]. Proton-sensitive reactions can be controlled in space and time by PAGs which also provide a new method for converting light energy into chemical energy [11, 12]. PAGs can generally be activated by LED or visible light either in solution or the solid state [13], which makes PAGs applicable

to controlling various proton transfer processes, such as acid-catalyzed reactions [14–16], enzyme activity [17], biological probing [18], bacteria killing [19], etc.. Although the acid release properties of PAGs have been studied, there have been few PAGs with fluorescence response. Therefore, the development of new PAGs with fluorescence response is still a work of great significance.

Boron dipyrromethene (BODIPY) dyes have characteristics such as large molar absorption coefficient, high fluorescence quantum yield and easy modification [20–24]. If boron dipyrromethene (BODIPY) dyes could be potential photoacids, a sensitive method for the measurement of in-site produced proton will be developed. In this work, a BODIPY conjugated sulfonate (BDP-S) was reported as a fluorescence responsive photoacid. The light-induced emission changes, photoacid generation and antibacterial activity were studied.

Experimental

Chemicals and Measurements

All chemicals were purchased from commercial suppliers and were used without further purification. 2,4-dimethylpyrrole, *p*-hydroxybenzaldehyde, trifluoroacetic acid (TFA), 2,3-dichloro-5,6-dicyano-1,4-benzoquinone (DDQ), *p*-nitrobenzenesulfonyl chloride, 4-nitro- α -toluenesulfonyl

✉ Qiu-Yun Chen
chenqy@ujs.edu.cn

✉ Ling-Ling Qu
llqu@ujs.edu.cn

¹ School of Chemistry and Chemical Engineering, Jiangsu University, Zhenjiang, China

chloride, rhodamine B base and other chemicals were purchased from Energy Chemical Reagent Co., Ltd. 4-(5,5-Difluoro-1,3,7,9-tetramethyl-5H-4 λ^4 ,5 λ^4 -dipyrrolo[1,2-c:2',1'-f][1,3,2]diazaborinin-10-yl)phenol (BDP-OH) was synthesized according to the reported procedure [25].

The electronic absorption spectra were measured at room temperature by a UV-2450 UV–vis spectrophotometer. Fluorescence measurements were carried out on a fluorescence spectrofluorometer Model CARY Eclipse (VARIAN, USA), a 1.0 cm quartz cell (slit width = 5 nm). The ^1H NMR (400 MHz) and ^{13}C NMR (100 MHz) data was recorded on a Bruker AVANCE II 400 MHz spectrometer using CDCl_3 as a solvent. The chemical shifts (δ) were reported in ppm and coupling constants (J) in Hz. The pH of solution was measured using a Fisher Scientific Accumet AR15 benchtop meter and a pH combination electrode.

Synthesis of 4-(5,5-difluoro-1,3,7,9-tetramethyl-5H-4 λ^4 ,5 λ^4 -Dipyrrolo[1,2-c:2',1'-f][1,3,2]diazaborinin-10-yl)phenyl 4-nitrobenzenesulfonate (BDP-S)

To a solution of BDP-OH (170 mg, 0.5 mmol) and triethylamine (140 μL , 1 mmol) in dry DCM (10 mL) was added *p*-nitrobenzenesulfonyl chloride (133 mg, 0.6 mmol) dropwise at 0 $^\circ\text{C}$ under nitrogen. The reaction mixture was stirred for 4 h at room temperature. The solvent was then washed with saturated sodium chloride (3×10 mL), dried with sodium sulfate and concentrated *in vacuo*. The residue was loaded onto a column of silica gel to give BDP-S (219 mg, 83.5% yield) as an orange solid. ^1H NMR (400 MHz, CDCl_3) δ 8.38 (d, $J=8.8$ Hz, 2H), 8.05 (d, $J=8.8$ Hz, 2H), 7.28 (d, $J=8.5$ Hz, 2H), 7.19 (d, $J=8.5$ Hz, 2H),

6.01 (s, 2H), 2.55 (s, 6H), 1.33 (s, 6H). ^{13}C NMR (100 MHz, CDCl_3) δ 156.22, 151.14, 149.67, 142.44, 140.42, 139.24, 134.75, 131.12, 130.03, 129.97, 124.37, 123.05, 121.66, 14.60, 14.49.

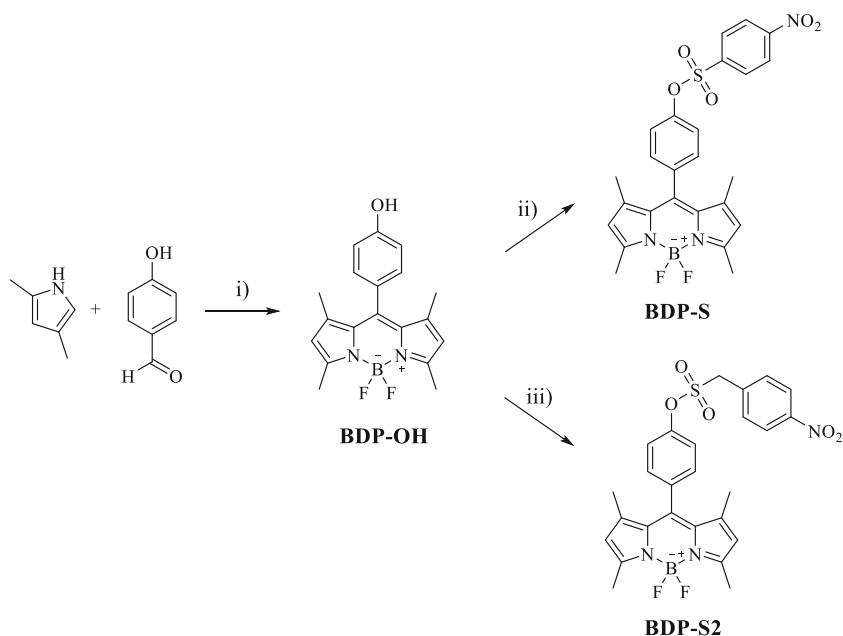
Synthesis of 4-(5,5-difluoro-1,3,7,9-tetramethyl-5H-4 λ^4 ,5 λ^4 -dipyrrolo[1,2-c:2',1'-f][1,3,2]diazaborinin-10-yl)phenyl (4-nitrophenyl)methanesulfonate (BDP-S2)

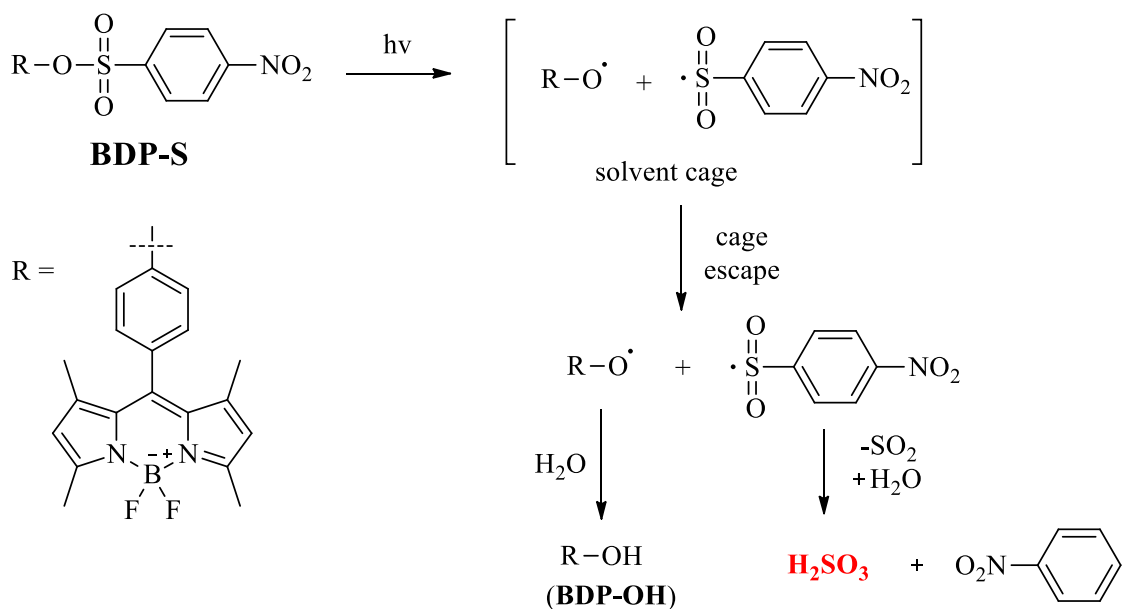
To a solution of BDP-OH (170 mg, 0.5 mmol) and triethylamine (140 μL , 1 mmol) in dry DCM (10 mL) was added 4-nitro- α -toluenesulfonyl chloride (141 mg, 0.6 mmol) dropwise at 0 $^\circ\text{C}$ under nitrogen. The reaction mixture was stirred for 10 h at room temperature. The solvent was washed with saturated sodium chloride (3×10 mL), dried with sodium sulfate and concentrated *in vacuo*. The residue was loaded onto a column of silica gel to give BDP-S2 (235 mg, 87.1% yield) as an orange solid. ^1H NMR (400 MHz, CDCl_3) δ 8.36 (d, $J=8.7$ Hz, 2H), 7.75 (d, $J=8.7$ Hz, 2H), 7.37 (q, $J=8.8$ Hz, 4H), 6.04 (s, 2H), 4.72 (s, 2H), 2.60 (s, 6H), 1.42 (s, 6H). ^{13}C NMR (100 MHz, CDCl_3) δ 156.13, 149.06, 148.63, 142.77, 139.48, 134.44, 134.12, 131.88, 131.22, 130.04, 124.20, 122.76, 121.60, 56.43, 14.60, 14.52.

Detection of H^+ Formed By Photolysis

The photogenerated acid (H^+) was captured by the added rhodamine B base whose lactone ring will open after accepting a proton, with a new absorption peak rising at 555 nm [26]. A solution of BDP-S or BDP-S2 (1 mM, MeCN) and rhodamine B base (20 μM , MeCN) was degassed with nitrogen for 15 min and irradiated with an LED lamp (365 nm,

Scheme 1 Schematic illustration of antibacterial mechanism for photoacid





Scheme 2 The mechanism for the photolysis of BDP-S

10 mW/cm²) for 2 h. The UV-Vis spectrum of the solution was recorded every 20 min. A rhodamine B base solution without BODIPY was used as a negative control.

Fluorescence Emission and PH Changes Under Irradiation

A BDP-S or BDP-S2 stock solution (70 μM, MeCN) was nitrogen saturated for about 15 min firstly and then irradiated with white LED lamps (350–500 nm, 4 mW/cm²) for 2 h. Photolysis process of BDP-S and BDP-S2 was monitored by fluorescence spectra (λ_{ex}: 480 nm, time interval: 20 min). The pH of the solution after different exposure times were measured by a Fisher Scientific Accumet AR15 benchtop meter and a pH combination electrode. For determining the changes

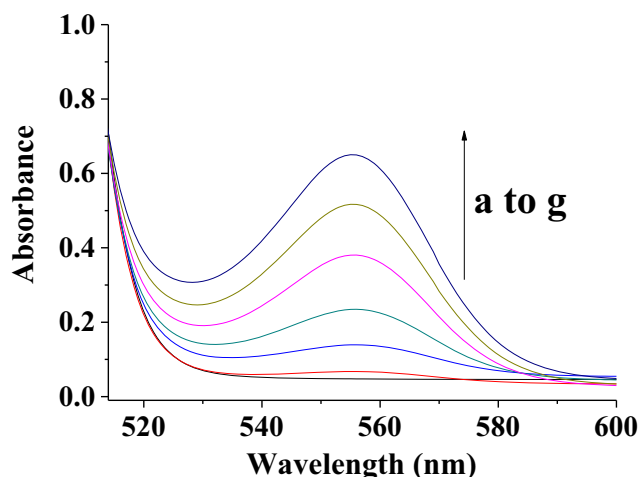


Fig. 1 UV-Vis spectra changes of BDP-S (500 μM, MeCN) and RB Base (10 μM, MeCN) mixture irradiated under 365 nm (a to g: 0 to 120 min, time interval: 20 min)

of emission and pH, three independent experiments were carried out.

Antibacterial Assays

Gram-negative *Escherichia coli* (*E. coli*, ATCC 25,922) strain was chosen as a standard bacterial model. The antibacterial activity of BDP-S was evaluated in the dark condition or LED light irradiation. All assays were conducted in 96-well, flat bottom, sterile plates. Bacterial suspension was adjusted to contain 1×10^6 CFU/mL in fresh sterile PBS solution. The as-prepared BDP-S solution (50, 40, 30, 20, 10 and 0 μM) was mixed with bacterial suspension (1×10^6 CFU/mL) and irradiated using a white LED lamp (35–500 nm, 4 mW/cm²) for 2 h. For each test, the sample in a dark was set as a control group. All tests were performed in triplicate. Survivors were quantified using the viable count technique. Plates were incubated at 37 °C for 24 h.

Results and Discussion

Syntheses and Characterization of Compounds

Two new BODIPY derivatives (BDP-S and BDP-S2) were synthesized by simply coupling hydroxyl-conjugated BODIPY (BDP-OH) with *p*-nitrobenzenesulfonyl chloride or 4-nitro- α -toluenesulfonyl chloride (Scheme 1). The ¹H NMR and ¹³C NMR spectra of the compounds confirm the compounds with exact structures and high purity (Figure S1–S6). BDP-S was found to decompose upon irradiation between the two compounds, whilst the pH of the solution was changed. A mechanism for the photolysis of BDP-S is

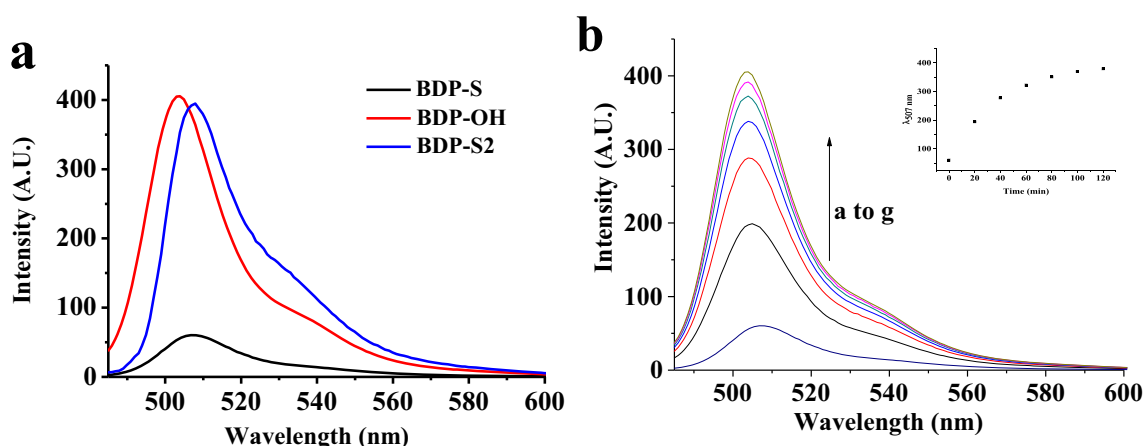


Fig. 2 **a** Fluorescence emission spectra of BDP-OH (70 μ M, MeCN), BDP-S (70 μ M, MeCN) and BDP-S2 (70 μ M, MeCN); **b** Fluorescence emission spectra changes of BDP-S (70 μ M, MeCN) irradiated with

white LED light (a to g: 0 to 120 min. Time interval: 20 min. Insert: changes of intensity at 507 nm). Excitation wavelength: 480 nm, Voltage: 500V

outlined in Scheme 2. After initial excitation, BDP-S undergoes homolytic O-S bond cleavage to generate phenoxyl and sulfonyl radical pairs [11]. The generated radical pairs, escape from the cage and subsequently abstract trace water or releases SO_2 to produce the corresponding BDP-OH and H_2SO_3 .

gradually changed from light yellow to a final light orange colour (Fig. S7). When the rhodamine B base was dissolved in acetonitrile, it is colorless, whilst its protonated form is red. The result also showed that rhodamine B base captured protons during LED irradiation and indirectly proved the release of acid species by BDP-S.

Detection of H^+ Formed By Photolysis

The generated H^+ was captured by rhodamine B base [25]. Protonation of rhodamine B base leads to a new peak arising at 555 nm. As shown in Fig. 1, a new peak rose gradually at 555 nm in the mixed solution of BDP-S and rhodamine B base while BDP-S2 and the control group showed no significant changes, indicating that an acid species was produced after BDP-S was illuminated.

In addition, with the extension of irradiation time, the color of the mixed solution of BDP-S and rhodamine B base

Fluorescence Emission and pH Changes of BDP-S After Illumination

BODIPY dyes have the characteristics of large molar absorption coefficient and high photostability of the core while the nitrosulfonate-conjugated one is generally not stable. As shown in Fig. 2a, the integrated area of BDP-OH in the range of 485–600 nm is 7.12 ± 0.02 times higher than BDP-S and 0.98 ± 0.01 times higher than BDP-S2 under the same condition. BDP-S2 shows no significant changes in emission compared with BDP-OH while the emission of BDP-S is greatly

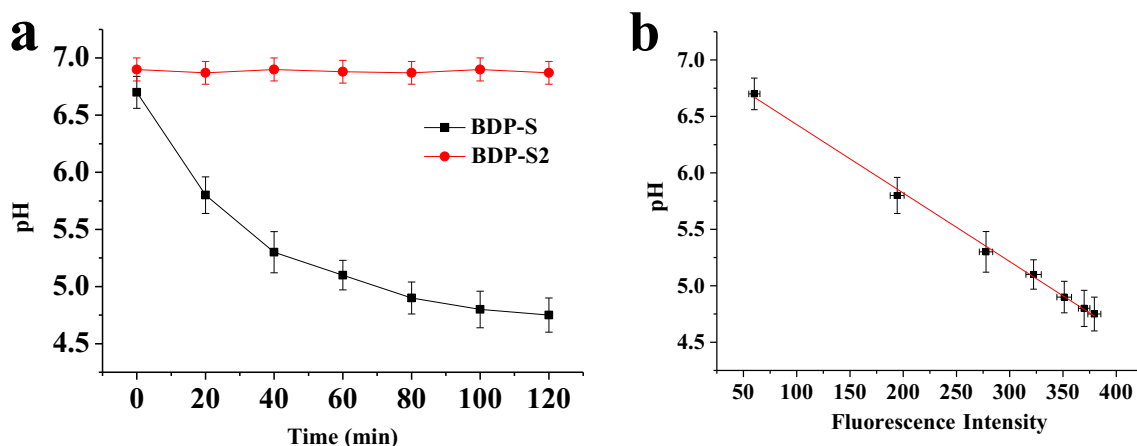
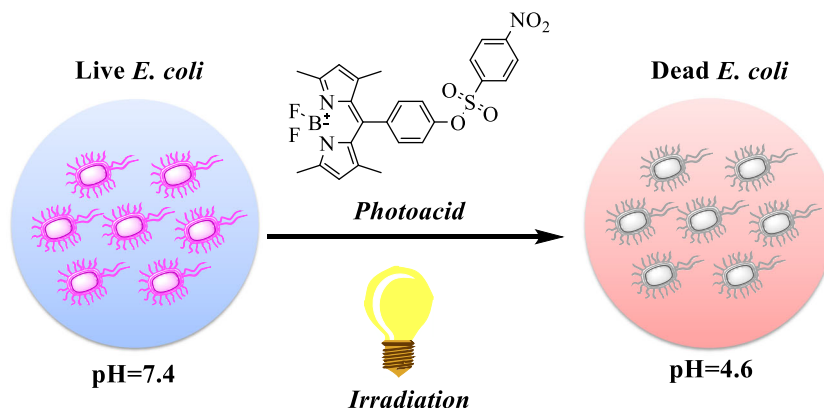


Fig. 3 **a** pH changes of BDP-S and BDP-S2 under illumination. **b** A fitted curve according to the measured pH and fluorescence intensity of BDP-S ($y = -0.00607 * x + 7.03523$, $R^2 = 0.997$). Data are expressed as the means of three independent experiments \pm SD

Scheme 3 Schematic illustration of antibacterial mechanism for photoacid



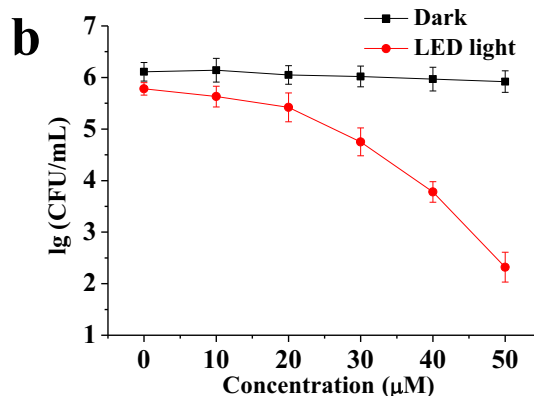
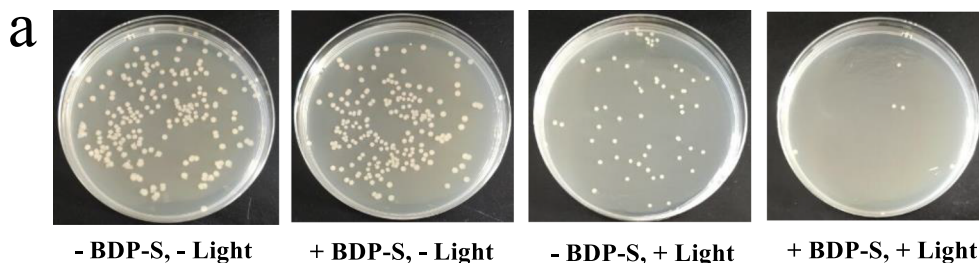
quenched, indicating that the methylene group in BDP-S2 breaks the conjugated structure and blocks the electron-withdrawing effect of the nitro group on BODIPY core. The emission of BDP-S2 shows no obvious change under long-term illumination while emission intensity of BDP-S at 507 nm increases with the extension of the illumination time and the amplitude decreases (Fig. 2b). Furthermore, BDP-S can be a fluorescence-response photo-acid. Besides, there is a slight blue shift (508 nm → 504 nm) observed that further proves that the structure of BDP-S changes under illumination.

Also, the pH of the solution under different exposure times was measured using a Fisher Scientific Accumet AR15 bench-top meter with a pH combination electrode (Fig. 3a). The results showed that the pH value of the BDP-S2 solution remained basically unchanged under illumination, while the

photolysis of BDP-S occurred and the pH of the solution decreased significantly with the exposure time. A curve based on the pH value and fluorescence intensity of BDP-S was fitted (linear regression equation: $y = -0.00607 * a + 7.03523$, $R^2 = 0.997$) (Fig. 3b), which allows us to roughly estimate of the pH value of the irradiated solution according to fluorescence emission intensity. Since the pH is the negative logarithm of the hydrogen ion concentration, the number of protons in solution can be easily calculated, which provides a new method for estimating the number of protons in a hydrophobic environment. This makes BDP-S a fluorescent visual proton donor.

Increasing acidity is an effective method for bacterial inactivation by inhibiting the synthesis of intracellular proteins at low pH. Since BDP-S can lower the pH of the solution with light, it can be applied for bacterial inactivation.

Fig. 4 a Growth of *E. coli* under different conditions (concentration of BDP-S: 50 μM); b Effects of increasing concentrations of BDP-S on the growth inhibition of *E. coli*. Data are expressed as the means of three independent experiments ± SD. The white light source (350–500 nm, 4 mW/cm²)



The proposed antibacterial mechanism for photoacid is outlined in Scheme 3.

Antibacterial Assays

The antibacterial activity of BDP-S was evaluated in the dark condition or under white LED light irradiation. As shown in Fig. 4a, the bacteria can grow normally in the dark condition (-BDP-S, -light) and the addition of BDP-S has limited effects on its growth (+BDP-S, -light). The number of survivors drops dramatically after *E. coli* is irradiated with white LED light (-BDP-S, +light) compared to the group without light (-BDP-S, -light). The number of bacteria drops after the addition of BDP-S under irradiation, indicating that the BDP-S caused a reduction in the number of bacteria. The light-driven antibacterial activity of BDP-S depends on its concentration. The number of survivors was reduced by 3 log units when the concentration of BDP-S was increased from 0 to 50 μM (Fig. 4b). The results indicate that BDP-S has the potential to be an excellent photoacid sterilizer.

Conclusions

Two BODIPY sulfonates (BDP-S and BDP-S2) were characterized by spectroscopic methods. The emission changes, acid generation and antibacterial activity on *E. coli* were studied in depth. BDP-S was found to lower the pH of the solution under illumination, which makes it a kind of hydrophobic proton donor. Light-induced antibacterial results indicate that BDP-S has a high inhibitory effect on the growth of *E. coli*. Our research results demonstrate that BDP-S is a very promising photoacid sterilant.

Supplementary Information The online version contains supplementary material available at <https://doi.org/10.1007/s10895-021-02682-8>.

Acknowledgements This work was financially supported by the National Natural Science Foundation of China (21701056).

Author Contributions All authors contributed to the study conception and design. Conceptualization: Qiu-Yun Chen; Methodology: Ling-Ling Qu; Formal analysis and investigation: Abbas Mohammed Ali, Jian Shao, Jia-Xin Wang and Yang Li; Writing- original draft preparation: Abbas Mohammed Ali; Writing - review and editing: Qiu-Yun Chen and Ling-Ling Qu; Funding acquisition: Ling-Ling Qu; Supervision: Qiu-Yun Chen.

Funding This work was financially supported by the National Natural Science Foundation of China (21,701,056).

Data Availability The data used to support the findings of this study are included within the article.

Compliance with Ethical Standards

Conflict of Interest The authors declare that there is no conflict of interest.

References

1. Stuart B, Bonnie M (2004) Antibacterial resistance worldwide: causes, challenges and responses. *Nat Med* 10:122–129
2. Kieron O, James H, Hannah S, Martin W, George S, David S (2013) Combating multidrug-resistant bacterial: current strategies for the discovery of novel antibacterials. *Angew Chem Int Ed* 52: 10706–10733
3. Kim CB, Yi DK, Seung P, Soo K, Lee W, Kim MJ (2009) Rapid photothermal lysis of the pathogenic bacteria, *Escherichia coli* using synthesis of gold nanorods. *J Nansci Nanotechnol* 9:2841–2845
4. Lu JY, Zhang PL, Chen QY (2019) A nano-BODIPY encapsulated zeolitic imidazolate framework as photoresponsive integrating antibacterial agent. *ACS Appl Bio Mater* 3:458–465
5. Luo Y, Wang C, Peng P, Hossain M, Jiang T, Fu Wl, Liao Y, Su M (2013) Visible light mediated killing of multidrug-resistant bacteria using photoacids. *J Mater Chem B* 1:997–1001
6. Amdursky N, Simkovitch R, Huppert D (2014) Excited-state proton transfer of photoacids adsorbed on biomaterials. *J Phys Chem B* 118:13859–13869
7. Haghghat S, Ostresh S, Dawlaty J (2016) Controlling proton conductivity with light: a scheme based on photoacid doping of materials. *J Phys Chem B* 120:1002–1007
8. Escuin R, Luisa M, Vaca G, Carbonell J, Luis J, Pedro AS (1983) A study of the photochemical response of *o*-nitrobenzyl cholate derivatives in P(MMA-MAA) matrices. *J Poly Sci : Poly Chem Ed* 21:1075–1083
9. Tsuguo Y, Hirosh A, Kazuo M, Hiroo W, Tsutomu S (1990) Photochemical dissociation of *p*-nitrobenzyl 9,10-dimethoxyanthracene-2-sulphonate via intramolecular electron transfer. *J Chem Soc Perkin Trans II* 2:1709–1714
10. Arnold A, Fratesi E, Bejan E, Cameron J, Pohlert G, Liu H, Scaiano J (2004) Evidence of homolytic and heterolytic pathways in the photodissociation of iminosulfonates and direct detection of the *p*-toluenesulfonyloxyl radical. *Photochem Photobiol Sci* 3:864–869
11. Ditkovich J, Mukra T, Pines D, Huppert D, Pines E (2015) Bifunctional photoacids: remote protonation affecting chemical reactivity. *J Phys Chem B* 119:2690–2701
12. Andraos J, Barclay G, Medeiros D, Baldovi M, Scaiano J, Sinta R (1998) Model studies on the photochemistry of phenolic sulfonate photoacid generators. *Chem Mater* 10:1694–1699
13. Martina C, Rapenneab G, Nakashimac T, Kawai T (2018) Recent progress in development of photoacid generators. *J Photochem Photobiol C: Photochem Rev* 34:41–51
14. Shi Z, Peng P, Strohecker D, Liao Y (2011) Long-lived photoacid based upon a photochromic reaction. *J Am Chem Soc* 133:14699–14703
15. Fu C, Xu J, Boyer C (2016) Photoacid-mediated ring opening polymerization driven by visible light. *Chem Comm* 52:7126–7129
16. Huang DL, Fang XL, Chen QY, Gao J (2018) Polymer united Fe_3O_2 nanospheroids for water oxidation and the green synthesis of 2,3-dihydrophathazine-1,4-dione. *ACS Sustain Chem Eng* 6: 11280–11285
17. Xia Y, Peng L (2013) Photoactivatable lipid probes for studying biomembranes by photoaffinity labeling. *Chem Rev* 11:37880–37929

18. Xu J, Shen X, Jia L, Zhang C, Zhou T, Zhu T, Xu Z, Cao J (2018) A ratiometric nanosensor based on lanthanide-functionalized attapulgite nanoparticle for rapid and sensitive detection of bacterial. *Dye Pigment* 148:44–51
19. Zhu X, Zhu Z (2018) The generalized predictive control of bacteria concentration in marine lysozyme fermentation process. *Food Sci Nutr* 7:1387–1395
20. Shao J, Chen QY, Zheng QL (2020) Nano adamantane-conjugated BODIPY for lipase affinity and light driven antibacterial. *Spectrochim Acta A* 234:118252–118255
21. Zhang PL, Shao J, Chen QY, Qu LL (2019) A protein amantadine-BODIPY assembly as a turn-on sensor for free copper(II). *Analy Methods* 11:827–831
22. Saravanan V, Rajakumar P (2018) Synthesis, characterization, optical and electrochemical properties and antibacterial activity of novel BODIPY glycoconjugated dendrimers. *New J Chem* 42: 2504–2512
23. Li Z, Zhu Z, Sun Z, Ding J, You J (2019) Design of a multifunctional biotinylated copper complex for visualization and quantification of cancer hypoxia levels. *Sens Actuators B Chem* 282:541–548
24. Zhang PL, Chen QY, Du X, Gao J (2019) Biocompatible-G-quadruplex/BODIPY assembly for cancer cell imaging and the attenuation of mitochondria. *Bioorg Med Chem Lett* 29:1943–1947
25. Fu YJ, Li Z, Li CY, Li YF, Wen LH (2017) Borondipyrrolemethene-based fluorescent probe for distinguishing cysteine from biological thiols and its application in cell image. *Dyes Pigments* 139:381–387
26. Pohlers G, Scaiano J, Sinta R (1997) A novel photometric method for the determination of photoacid generation efficiencies using benzothiazole and xanthene dyes as acid sensors. *Chem Mater* 9: 3222–3230

Publisher's Note Springer Nature remains neutral with regard to jurisdictional claims in published maps and institutional affiliations.